This is a post-peer-review, pre-copyedit version of an article published in IEEE Transactions on Antennas and Propagation. The final authenticated version is available online at: https://doi.org/10.1109/TAP.2017.2684198

Efficient Complex Root Tracing Algorithm for Propagation and Radiation Problems

Piotr Kowalczyk and Wojciech Marynowski, *Member, IEEE*

***Abstract*— An efficient complex root tracing algorithm for propagation and radiation problems is presented. The proposed approach is based on a discretization of Cauchy's Argument Principle and its generalization to the $\mathbb{C} \times \mathbb{R}$ space. Moreover, an engagement of the tracing process with a global root finding algorithm recently presented in the literature is performed. In order to confirm a validity and efficiency of the proposed technique, a few different types of structures have been analyzed.**

***Index Terms*— Complex modes, complex root finding, complex root tracing, graphene transmission line, resonant structures.**

I. Introduction

THE propagation and radiation problems are usually analyzed in a complex domain. The main parameter γ (propagation coefficient), which describes basic properties of waveguides, is a complex number and simultaneously represents losses, radiation, or even complicated wave types in shielded lossless structures (complex modes). On the other hand, antennas impedances or resonant frequencies of resonators are also complex. Therefore, the analysis of all such issues in a complex domain is much more convenient than in a real one.

In many cases, the analysis boils down to finding a complex root of a function $F(z) = 0$, where z can represent a propagation coefficient, a resonant frequency, or any other parameter. For instance, the function can be obtained directly from a set of equations (e.g., boundary conditions) or from an eigenvalue problem (e.g., free of sources analysis). Moreover, $F(z) = 0$ can be expressed in analytical (e.g., mode matching technique) or numerical terms (e.g., spectral domain approach) and evaluation of such function can be very time-consuming.

In many cases, the analysis must be performed in a function of some extra parameter t, then the problem can be expressed involving a function of two variables

$$F(z, t) = 0. \tag{1}$$

For instance, a dispersion characteristic of a waveguide is a function of frequency; resonant frequency can be a function of a dimension or some material property. Therefore, the analysis is performed many times for different values of the extra parameter, which can be tedious and time-consuming. In such cases, an algorithm, which traces the root in a function of the extra parameter, can be very efficient. This approach has been proposed and successfully applied in a real domain [1] and in a complex domain also [2], [3]. In these publications, the main idea of the tracing is based on checking the sign changes of the function in new systematically evaluated points. The new point is added in a vertex of equilateral triangle (in 2-D), in a vertex of tetrahedron (in 3-D), or in a vertex of pentachoron (in 4-D). An example of the algorithm for 2-D real case is presented in Fig. 1. The process starts from a segment (two points located at the x-axis) on which the function $F(x, y)$ changes its sign. In the first step, a new point is added at the vertex of the equilateral triangle. The function sign is then checked, and one of the triangle arms (the one with different signs at the ends) becomes a starting segment for the next step.

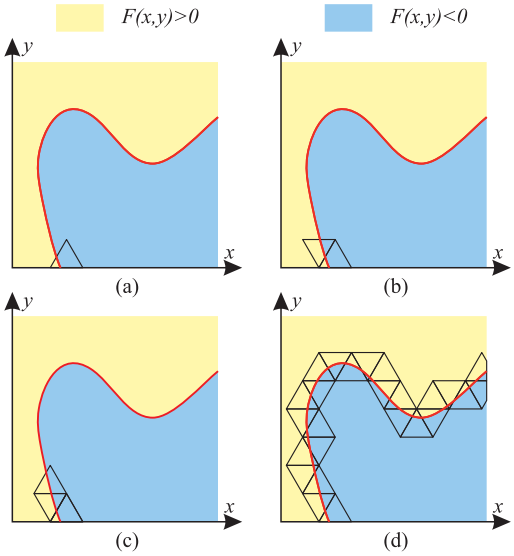

Fig. 1. Example of a root tracing process in real 2-D case [2], [3]. (a)–(c) First three steps. (d) Final result.

Unfortunately, while the technique can be successfully used in a real domain, it is ineffective in a complex domain. The idea of the scheme presented in [2] and [3] is insufficient—there is no guarantee that different signs of the real and the imaginary parts of the function imply a root inside the considered region. In Fig. 2, a few examples of the complex roots are presented, which contradict the assumption of the theory presented in [2] and [3]. In a complex domain, an unambiguous confirmation of the existence of the root in a fixed region is much more complicated.

In this paper, a modification of the method described in [2] and [3] is proposed, which enables the correct

This work was supported by the National Science Center under Grant DEC-2013/11/B/ST7/04309.

The authors were with the Department of Microwave and Antenna Engineering, Faculty of Electronics, Telecommunications, and Informatics, Gdańsk University of Technology, 80-233 Gdańsk, Poland

Digital Object Identifier 10.1109/TAP.2017.2684198

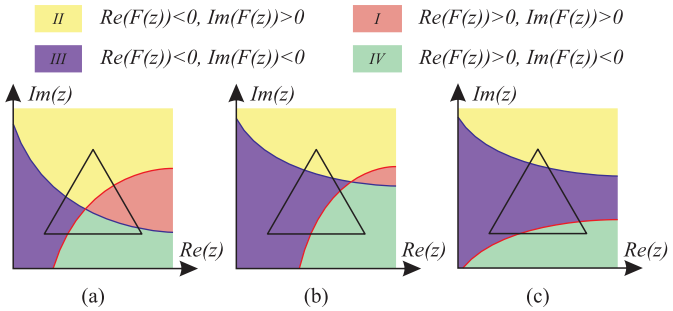

Fig. 2. Signs of the real and the imaginary parts of the functions are different in the vertices of the triangle. Root is located (a) inside and (b) outside the triangle. (c) There is no root in a close vicinity of the considered region.

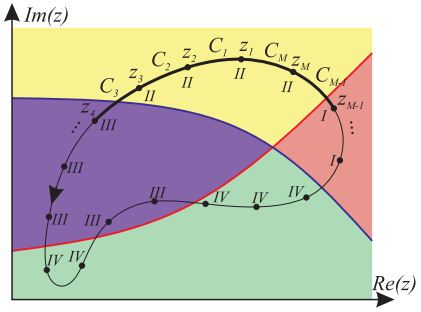

Fig. 3. Contour of integration (2). I–IV represents quadrants of a complex plane, which takes the function on this contour.

application of the algorithm in a complex domain. The proposed approach is based on Cauchy's Argument Principle [5], which is widely used in electromagnetics [6], as well as in control theory [7]. The principle is generalized to the $\mathbb{C} \times \mathbb{R}$ space and discretized with the minimal number of points (function evaluations) required to confirm the existence of the roots. Moreover, an engagement of the tracing process with a new global root finding algorithm recently presented in [4] is performed. The global algorithm concerns a complex domain only (fixed value of the parameter t), so it can be applied to provide all initial points, which are necessary to start the tracing root process. In this global technique, the function is approximated on the mesh, and the two curves representing the zeros of its real and imaginary parts are obtained. In turn, the "candidate points" are evaluated as intersections of these curves. Finally, these candidate points are verified and its accuracy can be improved. If the roots are located at the branch cut, a simple technique involving a pointwise product of all the Riemann surfaces can be applied [8].

The validity and efficiency of the proposed technique are supported by the results obtained from numerical tests for different types of electromagnetic problems.

II. Dicretization of Cauchy's Argument Principle

As it was mention before, in a complex domain, the confirmation of the existence of a root in the considered region is much more complicated than in a real domain. In order to verify the region, Cauchy's Argument Principle can be applied [5]. According to this principle, the integral

$$q = \frac{1}{2\pi i} \oint_C \frac{F'(z)}{F(z)} dz \tag{2}$$

represents a change in the argument of the function $F(z)$ over a closed contour C, which is a boundary of the considered region. In general, q is a sum of all zeros counted with their multiplicities, minus the sum of all poles counted with their multiplicities. If the region contains only one special point (root or singularity), the parameter q can be the following:

1) a positive integer—root of order q;
2) a negative integer—singularity of order $-q$;
3) zero—regular point.

The integral (2) may seem to be simple to solve, due to its trivial form (derivative of logarithm), even if it depends on the path of integration and must be directly evaluated. However, the complex logarithm definition of $w \in \mathbb{C}$ is not unique [5]

$$\log w = \log |w| + i \operatorname{Arg} w + 2n\pi i \tag{3}$$

where $n \in \mathbb{Z}$ can be arbitrary. Therefore, the parameter q could be any integral number. Even utilizing the principle value of the complex logarithm (with $n = 0$ and $\operatorname{Arg}(w) \in (-\pi, \pi]$), the result of the integration can be ambiguous, and the expression (2) requires a very special treatment.

In practice, it is convenient to divide the contour C into M segments $C = \bigcup_{m=1}^{M} C_m$ (see Fig. 3)

$$q = \frac{1}{2\pi i} \sum_{m=1}^{M} \int_{C_m} \frac{F'(z)}{F(z)} dz \tag{4}$$

then each of the integrals can be evaluated separately

$$q = \frac{1}{2\pi i} \left[\sum_{m=1}^{M-2} (\ln f(z_{m+1}) - \ln f(z_m)) + (\ln f(z_1) - \ln f(z_M)) \right]. \tag{5}$$

Utilizing definition (3), all the real parts of the sum terms in (5) can be reduced and

$$q = \frac{1}{2\pi} \sum_{m=1}^{M-2} \Theta_m \tag{6}$$

where

$$\Theta_m = \begin{array}{ll} \operatorname{Arg} f(z_{m+1}) - \operatorname{Arg} f(z_m), & m = 1, \ldots, M-1 \\ \operatorname{Arg} f(z_1) - \operatorname{Arg} f(z_m), & m = M \end{array} \tag{7}$$

represents changes in the argument of the function $F(z)$ over each segment C_m. To obtain the correct result, all the segments C_m must be sufficiently short, that $|\Theta_m| \leq \pi/2$. To this aim, the density of points can be systematically increased by adding the new points in the middle distances between the existing ones.

In Fig. 4, a few examples of the dicretized Cauchy's Argument Principle (single root, double root, and singularity). The function argument varies along the contour taking the values from the four quadrants (I, II, III, and IV). As can be observed, to obtain the proper result, none of the quadrant changes can be omitted. By summing all the increases in the quadrant

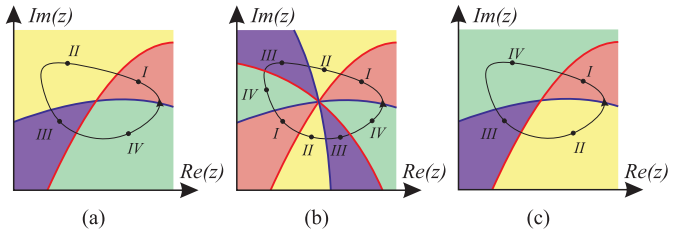

Fig. 4. Examples of discrertized Cauchy's Argument Principle. (a) Single root $q = 1$. (b) Double root $q = 2$. (c) Singularity $q = -1$.

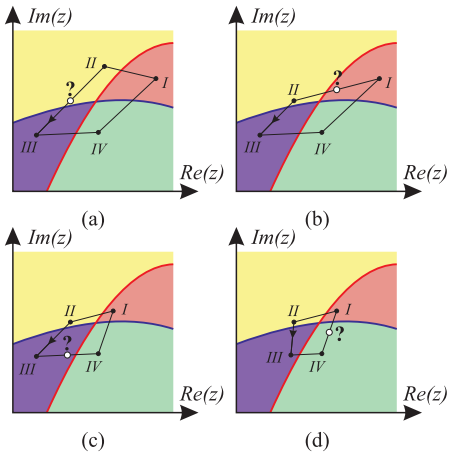

Fig. 5. Four steps of the generalized bisection method on a complex plane in the following sequence: from (a) to (d).

numbers along the contour in the counterclockwise direction, one obtains 4, 8, and -4, respectively. Hence, each change in the quadrant number represents changes in the function argument of $\pi/2$, so the parameter q is equal to 1, 2, and -1, respectively (single root, double root, and singularity).

A. Bisection on a Complex Plane

The discretization described above enables to construct an extension of the standard bisection method to a complex plane (see Fig. 5). As it is shown, for appropriately small region, only four points located in different quadrants (other points can be neglected) are sufficient to confirm the existence of the single root inside this region. In each step, a new point is added in the middle of the longest segment [see Fig. 5(a)]. The function value in this new point must be from the same quadrant as the one of the ends of the considered segment. Then the one of the ends of the segment (from the same quadrant) is removed. As the result, the considered region is reduced. The process can be repeated for the longest segment of the new contour, until the desired accuracy is obtained [see Fig. 5(b)–(d)].

The convergence rate of such process is lower than three points technique (e.g., Muller method [9]). However, the proposed method has one important advantage—it determines the region in which the root is located (in each step of the routine). Any other techniques do not provide such information, while this feature is crucial in the construction of the tracking algorithm.

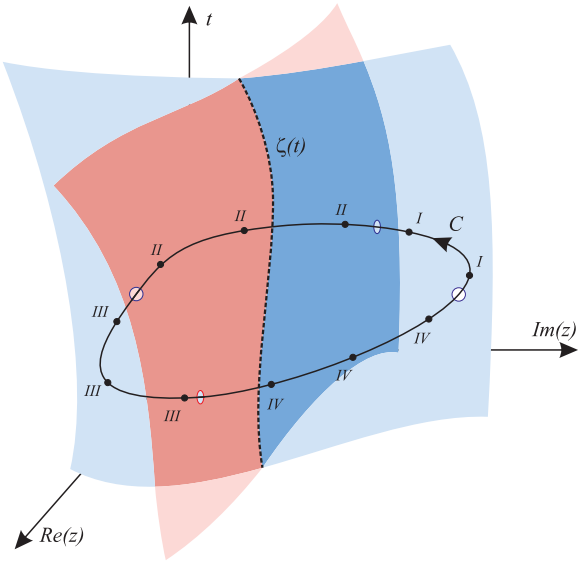

Fig. 6. Contour can be arbitrarily located in $\mathbb{C} \times \mathbb{R}$ space.

B. Generalization to $\mathbb{C} \times \mathbb{R}$ Space

Cauchy's Argument Principle has been originally proposed in a complex plane; however, its discrete modification can be directly generalized to $\mathbb{C} \times \mathbb{R}$ space. Let us consider the function $F(z, t)$, where $z \in \mathbb{C}$ and $t \in \mathbb{R}$. The root of $F(z, t) = 0$ can be a function of parameter t, then $F(\zeta(t), t) = 0$ where $\zeta(t)$ represents a curve in the considered $\mathbb{C} \times \mathbb{R}$ space (see Fig. 6).

In such case, if the contour C (not necessarily located in a plane $t = \text{const}$) surrounds the curve $\zeta(t)$, then the dicretized Cauchy's Argument Principle can be applied. Obviously, the values of parameter q have the same interpretation as in the previous paragraph.

III. Root Tracing Chain of Regular Tetrahedrons

In the tracing routine, the chain of regular tetrahedrons is constructed and the traced root must be enclosed inside this chain (see Fig. 7). To start the process, an initial point P is required. To this aim, the global algorithm [4] is applied. Then the point is surrounded by a contour (equilateral triangle) ABC presented in Fig. 7(a). The contour must contain at least four points representing different quadrants and they must be located in the correct sequence. Obviously, the vertexes of the triangle are not sufficient to fulfill this requirement. Hence, in the sequential steps, new points are added in the middle of the segments, until the condition is not met [see Fig. 7(b)].

In the next stage, a new point D is determined, so that establish a regular tetrahedron [see Fig. 7(c)]. Assuming a continuity of the $\zeta(t)$, the curve must intersect one of the side walls of the tetrahedron: ABD, BCD, or CAD. The process is then repeated starting from the wall, which contains the root (intersects with the curve $\zeta(t)$). It is possible that the condition of the different quadrants and the correct sequence is fulfilled at once on one of the walls [e.g., ABD in Fig. 7(c)]. However, in general, new points must be added at the segments AD, BD, and CD, until the condition is not met. Once again, it can be obtained by systematical increase of density

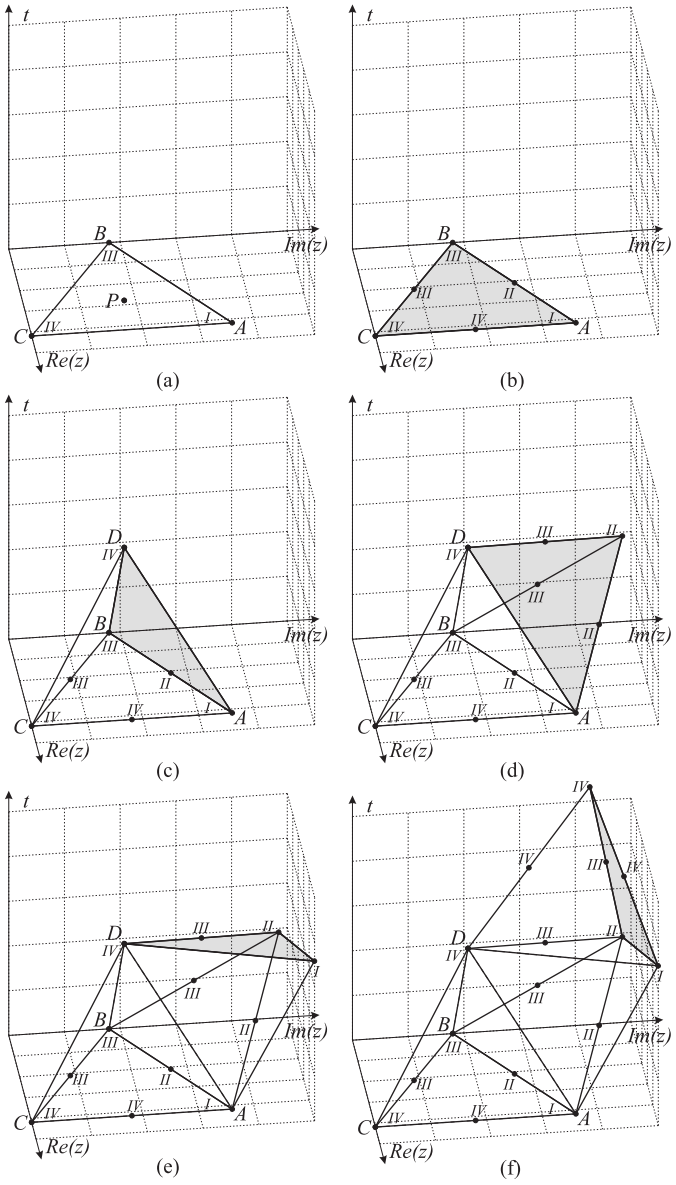

Fig. 7. Chain of regular tetrahedrons. (a) Initial point P surrounded by a contour (equilateral triangle) ABC. (b)–(f) The following steps of the tracing algorithm.

of points by placing the new points in the middle of the existing ones [see Fig. 7(d)]. In general, the total number of the new points (the function evaluations) cannot be determined *a priori*, but it depends on the edge length and the complexity of the function [see Fig. 7(e) and (f)].

The algorithm can be simply extended to trace singularities and roots of higher orders; however, in such cases, discrete Cauchy's Argument Principle requires greater number of points and the procedure has rather small practical importance.

IV. Numerical Results

In order to demonstrate the validity of the proposed method, three different structures are analyzed. The computational domain is assumed separately for each example. From the mathematical point of view, there are no restrictions on the choice of the computational domain bounds. In general, the domain can be arbitrary large; however, to improve the efficiency of the analysis, the domain should be as small as possible. In practice, the domain size depends on the considered structure. The more the information about the applications, principles of operation, and physical phenomena in the analyzed structure is known, the smaller the computational domain can be assumed. The tests are performed using Intel(R) Core i7-2600K CPU 3.40-GHz, 16-GB RAM.

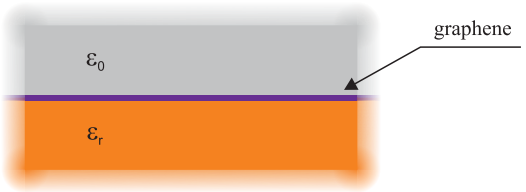

Fig. 8. Graphene transmission line, where $\varepsilon_r = 11.9$.

At first, a simple graphene transmission line is considered. The guide consists of a thin graphene layer deposited and a silicone substrate (see Fig. 8). An equivalent transmission-line model of the structures for TM modes is presented in [10]. Such approach involves spatial dispersion of the graphene [11]. In this case, the propagation characteristic can be found from the following equation:

$$F(\gamma, f) = \frac{\varepsilon_{r1}}{\eta_0\sqrt{\varepsilon_{r1}+\gamma^2}} + \frac{\varepsilon_{r2}}{\eta_0\ \overline{\varepsilon_{r2}+\gamma^2}} + \ \sigma_{\mathrm{lo}} - \gamma^2 k_0^2(\alpha_{\mathrm{sd}}+\beta_{\mathrm{sd}})\Big] \tag{8}$$

where γ is a normalized propagation coefficient (with respect to $k_0 = 2\pi f/c$), f represents frequency, and η_0 is a wave impedance of the vacuum. The graphene parameters depend on the frequency as follows:

$$\sigma_{\mathrm{lo}} = \frac{-iq_e^2 k_B T}{\pi\hbar^2(2\pi f - i\tau^{-1})} \ln\ 2\ \ 1+\cosh\ \ \frac{\mu_c}{k_B T}\Big)\Big)\Big] \tag{9}$$

$$\alpha_{\mathrm{sd}} = \frac{-3v_F^2\sigma_{\mathrm{lo}}}{4(2\pi f - i\tau^{-1})^2}, \quad \beta_{\mathrm{sd}} = \frac{\alpha_{\mathrm{sd}}}{3} \tag{10}$$

where q_e is the electron charge, k_B is Boltzmann's constant, $T = 300$ K, $\tau = 0.135$ ps, $\mu_c = 0.05q_e$, and $v_F = 10^6$ m/s.

The analysis is performed for the frequency range from 1 to 7 THz. The initial point is obtained from the global root finding algorithm [4] with a honeycomb arrangement of the mesh. The computational domain $\Omega = \{z \in \mathbb{C} : -400 < \mathrm{Re}(z) < 400 \wedge 0 < \mathrm{Im}(z) < 400\}$ is considered and the resolution Δr is assigned a value of 1. This step for frequency $f = 1$ THz results in two initial points (two modes) $\gamma = 336 + 285i$ and $\gamma = 32 + 27i$, which takes about 50 s of computations (371387 evaluations of the function). Then the tracing routine is performed with the same resolution step Δr (side length of the tetrahedron). To increase an efficiency of the process the frequency is normalized to 100 GHz. The final characteristic is shown in Fig. 9. The computational time of this step is significantly shorter; it takes only 10 s (372 437 function evaluations for both modes). Hence, the total analysis takes about 60 s. For comparison, the results of global analysis are presented in the characteristics (black asterisks).

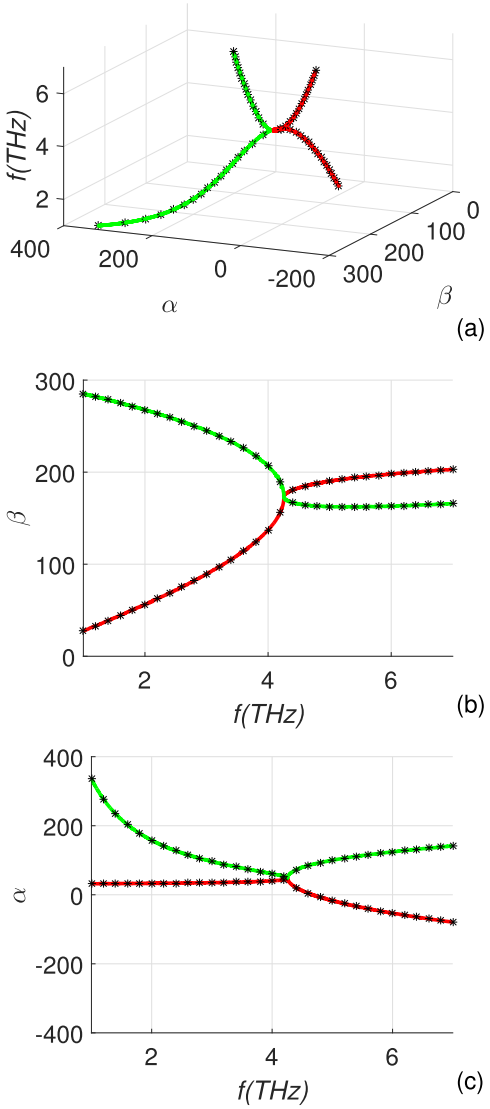

Fig. 9. Dispersion characteristics of two TM modes in the graphene transmission line. (a) General view. (b) Normalized phase coefficient. (c) Normalized attunuation coefficient.

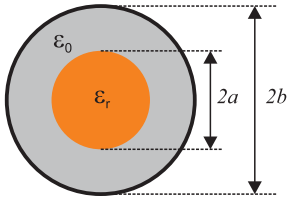

Fig. 10. Coaxially loaded cylindrical waveguide, where $\varepsilon_r = 10$, $a = 6.35$ mm, and $b = 10$ mm.

The 21 frequency points are sufficient to map the characteristic shape (this global analysis takes 1050 s, which is 17.5 times longer than the tracing process).

As the second example, a coaxially loaded cylindrical waveguide is considered [12]. In this structure, a very special type of waves can be guided—complex modes. The dimensions and parameters of the structure are presented in Fig. 10.

The propagation characteristic for this structure can be found directly from boundary conditions, by finding roots of the following determinant:

$$F(\gamma, f) = \begin{vmatrix} -J_1 & 0 & J_2 & Y_2 & 0 & 0 \\ 0 & J_1 & 0 & 0 & -J_2 & -Y_2 \\ -\frac{\gamma m J_1}{a\kappa_1^2} & -\frac{i\eta_0 J_1'}{\kappa_1} & \frac{\gamma m J_2}{a\kappa_2^2} & \frac{\gamma m Y_2}{a\kappa_2^2} & \frac{i\eta_0 J_2'}{\kappa_2} & \frac{i\eta_0 Y_2'}{\kappa_2} \\ -\frac{i\varepsilon_r J_1'}{\kappa_1\eta_0} & -\frac{\gamma m J_1}{a\kappa_1^2} & \frac{i J_2'}{\kappa_2\eta_0} & \frac{i Y_2'}{\kappa_2\eta_0} & \frac{\gamma m J_2}{a\kappa_2^2} & \frac{\gamma m Y_2}{a\kappa_2^2} \\ 0 & 0 & J_3 & Y_3 & 0 & 0 \\ 0 & 0 & \frac{\gamma m J_3}{b\kappa_2^2} & \frac{\gamma m Y_3}{b\kappa_2^2} & \frac{i\eta_0 J_3'}{\kappa_2} & \frac{i\eta_0 Y_3'}{\kappa_2} \end{vmatrix} \tag{11}$$

where γ represents a normalized propagation coefficient, f represents frequency, m is an angular variation, and η_0 is a wave impedance of the vacuum. The rest of coefficients are defined as follows: $J_1 = J_m(\kappa_1\, a)$, $Y_1 = Y_m(\kappa_1\, a)$, $J_2 = J_m(\kappa_2\, a)$, $Y_2 = Y_m(\kappa_2\, a)$, $J_3 = J_m(\kappa_2\, b)$, and $Y_3 = Y_m(\kappa_2\, b)$ (primes denote derivatives), whereas $\kappa_1 = k_0(z^2 + \varepsilon_r)^{1/2}$ and $\kappa_2 = k_0(z^2 + 1)^{1/2}$.

In this case, the analysis is performed for the frequency range from 3 to 7 GHz. As in the previous example, the initial points are obtained from the global algorithm. The computational domain $\Omega = \{z \in \mathbb{C} : -4 < \mathrm{Re}(z) < 4 \wedge -0.01 < \mathrm{Im}(z) < 4\}$ is considered and the resolution Δr is assigned a value of 0.01. This step (for frequency $f = 3$ GHz) results in two different points $\gamma = -2.93$ and $\gamma = 3.68$ (modes: EH_{11} and HE_{11}) and takes 95 s (372 312 evaluations of the function). Then the tracing routine is performed with the same resolution step Δr (side length of the tetrahedrons). This time, the frequency is normalized to 1 GHz. The final characteristics are shown in Fig. 11. The computational time of this step is also significantly shorter and takes only 24 s (177 133 function evaluations). Hence, the total analysis takes about 119 s. For comparison, the results of global analysis are presented in the characteristics (black asterisks). Due to a little bit more complicated characteristics, the global algorithm is run for 41 frequency points to map its shape, which takes about 3895 s (in this case, the global analysis is 33 times longer than the tracing process).

The last example is a cylindrical-rectangular microstrip resonant structure [13], which can be applied in conformal antennas [14]. The dimensions and parameters of the resonator are presented in Fig. 12. In this case, the spectral domain approach is used to estimate its resonant frequencies in a function of the air gap thickness s. The problem is formulated in terms of an integral equation using vector Fourier transforms. Then, applying Galerkins's method, the problem boils down to a homogeneous system of linear equations [13]

$$\boldsymbol{Z}\mathbf{I} = \mathbf{0} \tag{12}$$

where matrix $\boldsymbol{Z}$ depends on frequency f (which is a complex number $f = f_{\mathrm{Re}} + \mathrm{i}f_{\mathrm{Im}}$) and thickness s. To obtain nontrivial solution, the determinant of the matrix $\boldsymbol{Z}$ must be zero, hence

$$F(f, s) = \det(\boldsymbol{Z}). \tag{13}$$

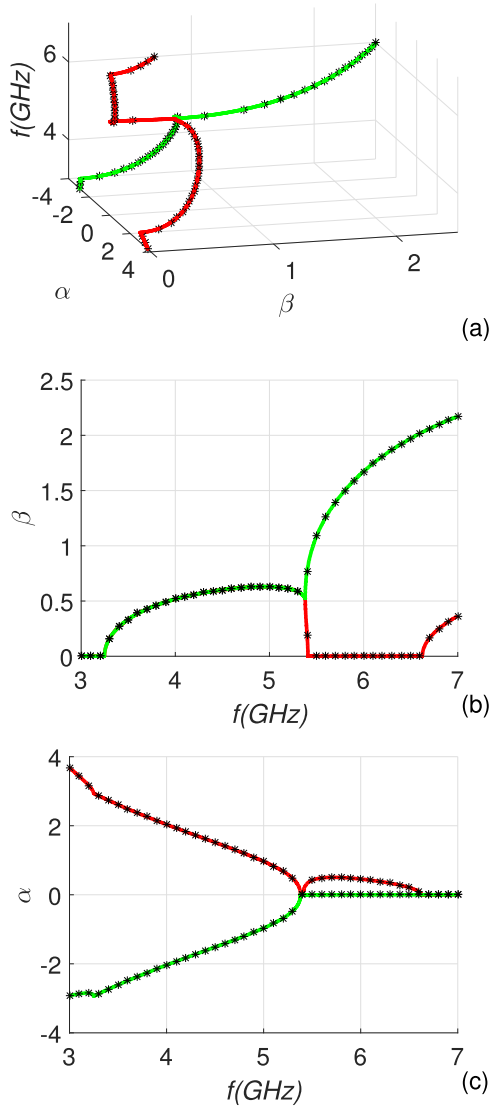

Fig. 11. Dispersion characteristics of EH_{11} and HE_{11} modes in a partially loaded waveguide. (a) General view. (b) Normalized phase coefficient. (c) Normalized attunuation coefficient.

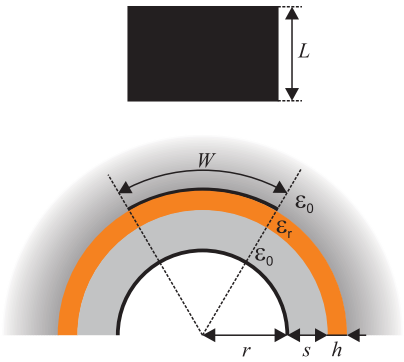

Fig. 12. Cylindrical-rectangular microstrip structure, where ground cylinder radius $r = 200$ mm, substrate permittivity $\varepsilon_r = 2.32$, and thickness $h = 2.4$ mm. Patch dimensions: $L = 80$ mm and $W = 168$ mm. Air gap of thickness s.

The analysis is performed for the thickness range from 0 to 10 mm. The initial point is obtained from the global root finding algorithm with the computational domain $\Omega = \{z \in \mathbb{C} : 1 < \mathrm{Re}(z) < 2 \wedge -0.2 < \mathrm{Im}(z) < 0\}$ and the

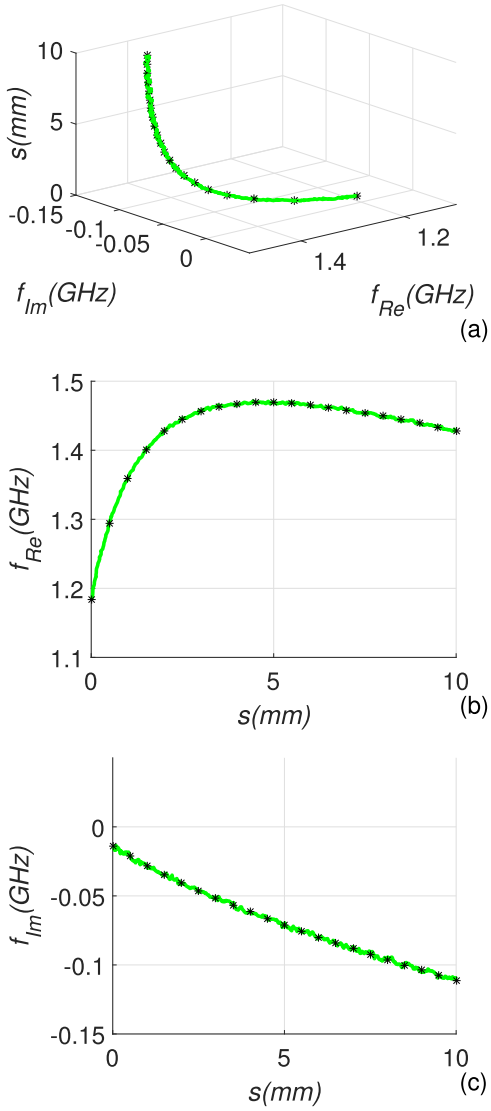

Fig. 13. Resonant frequency of the rectangular patch antenna on cylindrical surfaces. (a) General view. (b) Real part. (c) Imaginary part.

resolution $\Delta r = 0.01$. For parameter $s = 0$, the resonant frequency is $f = 1.18 - 0.01i$ GHz. This step takes about 2 h of computations (2592 evaluations of the function). Next, the tracing routine is performed with the same resolution step Δr (side length of the tetrahedrons). To increase an efficiency of the process, the thickness s is considered in millimeters. The changes of the resonant frequency are presented in Fig. 13. The computational time of the tracing process is about 4 h (6792 function evaluations), so the total analysis takes about 6 h. The results are compared with the ones obtained from global analysis (black asterisks). Due to a simple shape of the characteristic, only 21 thicknesses are considered (this global analysis takes about 42 h, which is seven times longer than the tracing process).

V. Conclusion

The numerical test confirms that the proposed algorithm is very simple, versatile, and efficient. The accuracy of the obtained characteristics (since its approximate value and char-

acter are known) can be quickly improved with the use of standard numerical method. The proposed method is an order of magnitude faster than global algorithm, and there is no need to segregate modes (as it must be done if the global algorithm is applied). These features are particularly important for optimization processes and can be successfully applied in many different types of technical problems.

ACKNOWLEDGMENT

The authors would like to thank Prof. J. Mazur and Dr. R. Lech for valuable suggestions and discussions on this paper.

REFERENCES

[1] M. Mrozowski, "An efficient algorithm for finding zeros of a real function of two variables," *IEEE Trans. Microw. Theory Techn.*, vol. 36, no. 3, pp. 601–604, Mar. 1988.

[2] J. J. Michalski and P. Kowalczyk, "Efficient and systematic solution of real and complex eigenvalue problems employing simplex chain vertices searching procedure," *IEEE Trans. Microw. Theory Techn.*, vol. 59, no. 9, pp. 2197–2205, Sep. 2011.

[3] J. Gulgowski and J. J. Michalski, "Topological attitude towards path following, applied to localization of complex dispersion characteristics for a lossy microwave, ferrite-coupled transmission line," *IMA J. Appl. Math.*, vol. 80, no. 2, pp. 494–507, 2015.

[4] P. Kowalczyk, "Complex root finding algorithm based on delaunay triangulation," *ACM Trans. Math. Softw.*, vol. 41, no. 3, pp. 19:1–19:13, Jun. 2015.

[5] J. W. Brown and R. V. Churchill, *Complex Variables and Applications*. New York, NY, USA: McGraw-Hill, 2009.

[6] W. Zieniutycz, "Comments on 'The ZEPLS program for solving characteristic equations of electromagnetic structures,'" *IEEE Trans. Microw. Theory Techn.*, vol. 31, no. 5, p. 420, May 1983.

[7] Y. S. Suh, "Stability of time delay systems using numerical computation of argument principles," in *Proc. 40th IEEE Conf. Decision Control*, Orlando, FL, USA, Dec. 2001, pp. 4738–4743.

[8] P. Kowalczyk, "On root finding algorithms for complex functions with branch cuts," *J. Comput. Appl. Math.*, vol. 314, pp. 1–9, Apr. 2017. [Online]. Available: http://dx.doi.org/10.1016/j.cam.2016.10.015

[9] G. W. Stewart, "On the convergence of multipoint iterations," *Numer. Math.*, vol. 68, no. 1, pp. 143–147, Jun. 1994.

[10] J. S. Gomez-Diaz, J. R. Mosig, and J. Perruisseau-Carrier, "Effect of spatial dispersion on surface waves propagating along graphene sheets," *IEEE Trans. Antennas Propag.*, vol. 61, no. 7, pp. 3589–3596, Jul. 2013.

[11] G. Lovat, P. Burghignoli, and R. Araneo, "Low-frequency dominant-mode propagation in spatially dispersive graphene nanowaveguides," *IEEE Trans. Electromagn. Compat.*, vol. 55, no. 2, pp. 328–333, Apr. 2013.

[12] M. Mrozowski, *Guided Electromagnetic Waves, Properties and Analysis*. Hoboken, NJ, USA: Wiley, 1997.

[13] K.-L. Wong, Y.-T. Cheng, and J.-S. Row, "Analysis of a cylindrical-rectangular microstrip structure with an airgap," *IEEE Trans. Microw. Theory Techn.*, vol. 42, no. 6, pp. 1032–1037, Jun. 1994.

[14] R. Lech, W. Marynowski, A. Kusiek, and J. Mazur, "An analysis of probe-fed rectangular patch antennas with multilayer and multipatch configurations on cylindrical surfaces," *IEEE Trans. Antennas Propag.*, vol. 62, no. 6, pp. 2935–2945, Jun. 2014.

Piotr Kowalczyk was born in Wejherowo, Poland, in 1977. He received the M.S. degree in applied physics and mathematics and the Ph.D. degree in electrical engineering from Gdańsk University of Technology, Gdańsk, Poland, in 2001 and 2008, respectively.

He is currently with Department of Microwave and Antenna Engineering, Technical University, Gdańsk. His current research interests include scattering and propagation of electromagnetic wave problems, algorithms, and numerical methods.

Wojciech Marynowski (M'16) was born in Bydgoszcz, Poland, in 1980. He received the M.Sc.E.E. and Ph.D. degrees from Gdańsk University of Technology, Gdańsk, Poland, in 2004 and 2011, respectively.

He is currently with Department of Microwave and Antenna Engineering, Technical University, Gdańsk. His research interests include electromagnetic wave propagation in complex materials, and design of nonreciprocal planar microwave devices, wideband/ultrawideband antennas, and theirs feeding systems.